A LOW CARBON ECONOMIC OPTIMAL DISPATCHING MODEL FOR COMPREHENSIVE ENERGY SYSTEM BASED ON IMPROVED WHALE ALGORITHM

Lin Jin* and Qian Sun**,***

Abstract

To optimise the scheduling model for the integrated energy system (IES), the paper proposes to introduce the combined cooling, heating, and power generation system into it, and proposes a reverse learning mechanism to improve the whale optimisation algorithm (WOA). The improved-algorithm optimized the comprehensive energy system of the cogeneration system. According to the results, the WOA converges in the 200th iteration with the reverse learning mechanism, while the original algorithm takes 400 iterations to converge. To introduce the carbon trading mechanism (CTM), it could cut down the operating costs and carbon emissions of the model. The lowest operating cost of introducing traditional CTMs is 1,889 yuan. The introduction of a tiered CTM resulted in the lowest carbon emissions of 2.15 t. To reduce operating costs, it is advisable to account for carbon emissions from electric energy storage (EES) equipment, especially before the carbon trading price reaches 102 yuan/t. After 102 yuan/t, calculating the carbon emissions of EES equipment can reduce operating costs. The model established through research does not link the carbon trading market with the electricity market, and can further explore the connections between the two markets. Further achieving the dual goals of low cost and low-carbon emissions provides strong support for achieving a green and low-carbon comprehensive energy system.

Key Words

Whale optimisation algorithm, energy system, CCHP, scheduling model, carbon trading

  * School of Finance and Trade, Wenzhou Business College, Wenzhou, China 325035
 ** School of Business Administration, Zhongnan University of Economics and Law, Wuhan, China 430073; e-mail: qiansun11@126.com
*** School of Finance and Economics, Wuhan College, Wuhan, China 430212
   Corresponding author: Qian Sun

1. Introduction

Achieving both low cost and low-carbon emissions is vital for promoting a sustainable and eco-friendly energy system. As the social and economic development continues, the consumption of non-renewable energy sources and the degradation of the ecological environment continues. It's becoming clear to people that it is urgent to protect the natural environment. Society cannot develop without carbon emissions, but the harm of carbon pollution to the ecological environment cannot be ignored. Reducing carbon emissions is necessary while balancing economic development. This has led to the emergence of a low-carbon economy [1]. This document proposes the key aspects of a low-carbon economy, drawn from the carbon trading theory, which refers to the emission rights of greenhouse gases and their tradability. Given the regulation of total carbon emissions, the greenhouse gas emission rights represent a limited resource that is tradable among carbon emitters and other entities, as it displays characteristics of a commodity [2]. After introducing this concept into the energy market, a new system of mutual restraint and balance has been formed between the carbon trading market and the energy trading market. At present, the energy industry is primarily focused on developing low-carbon energy options, with the aim of gradually reducing the market share of traditional petrochemical energy. Sources of low-carbon energy, such as electricity and thermal energy, are progressively gaining greater market share, thereby reducing the dominance of petrochemical energy within the energy system. However, it has created an integrated energy system (IES) [3] that incorporates various energy sources. The current stage of IES has not yet fully realised the interaction and collaborative control of the various energy sources incorporated in the system, which constrains its efficiency and reliability. Furthermore, current scheduling strategies commonly neglect the essential correlations between energy

sources and the energy market dynamics when managing multi-energy systems, thus impacting scheduling efficacy and system stability. To advance the advancement of low-carbon energy and diminish the carbon emissions of IES, a reverse learning mechanism was proposed to enhance the whale optimisation algorithm (WOA). The improved algorithm was used to study the optimal capacity configuration and carbon emission scheduling model of IES. The study will conduct research on the optimal scheduling model of IES from four parts. The first part is a review of the current research status of foreign IES systems and WOA. The second part proposes the construction method of IES optimal scheduling model, which is divided into two sections. The first section mainly introduces the composition of IES system, and the second section mainly introduces WOA and its improvement principle. The third part conducts experimental verification on the optimal scheduling model constructed in the study. The fourth part is a summary of the entire text.

2. Related Works

IES refers to a system where multiple energy sources are utilised in the same system to enhance energy economic efficiency by coordinating the proportion of each energy source's CE. Sakalis *et al.* proposed and designed an IES that covers all energy types on large crude oil transport ships to reduce the operating costs and environmental footprint of large crude oil transport ships. The model utilises net present value as the objective function, which enables the recovery of both high-pressure and low-pressure hot steam leading to an effective promotion of steam turbine, exhaust gas boiler, and auxiliary boiler [4]. To meet the diverse energy needs of customers, Yuan *et al.* upgraded their energy structure using the multi energy coupling utilisation platform provided by IES and proposed a multi-criteria decision-making way on the basis of IES. It is not only meets the demand for energy diversification but also improves energy utilisation efficiency [5]. Gao *et al.* proposed an optimisation planning framework that considers reliability to promote the sharing of user energy between the power grid and IES through market mechanisms. This framework established a price estimation model based on reliability theory to maximise the benefits of IES. The simulation experiment led by the author validated its effectiveness, analysed its influence in load growth rate and user reliability demands [6]. Su *et al.* proposed a new and robust calculation scheme to evaluate the safety of IES and derive the complete characteristics of its steady-state safety zone. This calculation method can eliminate the errors of existing methods and obtain complete steady-state safety zone features of IES [7]. Liu *et al.* constructed a new energy hub planning framework based on source load coordination. This framework can alleviate the natural benefits conflict in system economy and environment [8].

Guo *et al.* proposed a reverse learning and a flight disturbance strategy to optimise the WOA, and then utilised it to identify the parameters of the static reactive power compensator. It supports a new estimation way for precisely ensuring the static reactive power compensator model parameters [9]. Obadina *et al.* proposed a hybrid algorithm to optimise the robotic arm system of master–slave robots, which can effectively solve the parameter identification problem of robot models [10]. Gupta *et al.* proposed WOA to improve the recognition level of pressure in EEG signals and applied it to feature selection and extraction of EEG. This can complete a pressure recognition accuracy of 91% [11]. Kahya *et al.* established a feature selection method built on binary WOA to address the issue of the transfer function being unable to balance the exploration and development stages in the current formula. This method has different types of time-varying transfer function update techniques, which have consistency in feature selection, high classification accuracy, and better convergence [12]. Heraguemi *et al.* proposed an improved WOA for mining association rules to address the high computational cost of data mining technology. This algorithm is already superior to other swarm intelligence algorithms, *e.g.* quality, running time, and memory usage [13].

In summary, IES is currently the energy system with the lowest CE and the highest energy utilisation efficiency among all energy structures. However, its energy efficiency still needs improvement. WOA is an excellent heuristic algorithm that is commonly employed for parameter optimisation in various models. The objective of IES scheduling research is to optimise its parameters. However, the global search ability of IES is weak, and it is prone to falling into local optima. Thus, this study introduces a reverse learning mechanism to enhance WOA and utilises it to update IES system parameters to analyse the optimal scheduling module for the IES system.

3. Optimal CE Scheduling Model Based on Improved Whale Algorithm

Effective scheduling models can enhance economic efficiency and decrease CE. Chapter one primarily presents the tasks within each subsystem of IES along with corresponding mathematical models. Chapter two outlines the introduction of WOA and the reverse learning mechanism improvement strategy for WOA.

3.1 A Scheduling Module for Integrated Energy Systems

The energy of traditional power generation systems is mainly composed of non-renewable energy sources like coal and natural gas (NG), making it difficult to utilise the synergistic economic benefits between different energy sources. IES is a new approach that combines and complements multiple energy sources, and Fig. 1 illustrates its structure [14]–[16].

IES consists of three parts: the energy supply side, the energy conversion and storage side, and the user demand side. The combined cooling heating and power (CCHP) system is an emerging energy comprehensive tiered utilisation scheme in IES. The system consists of nine sub models: micro gas turbine, gas boiler, electric
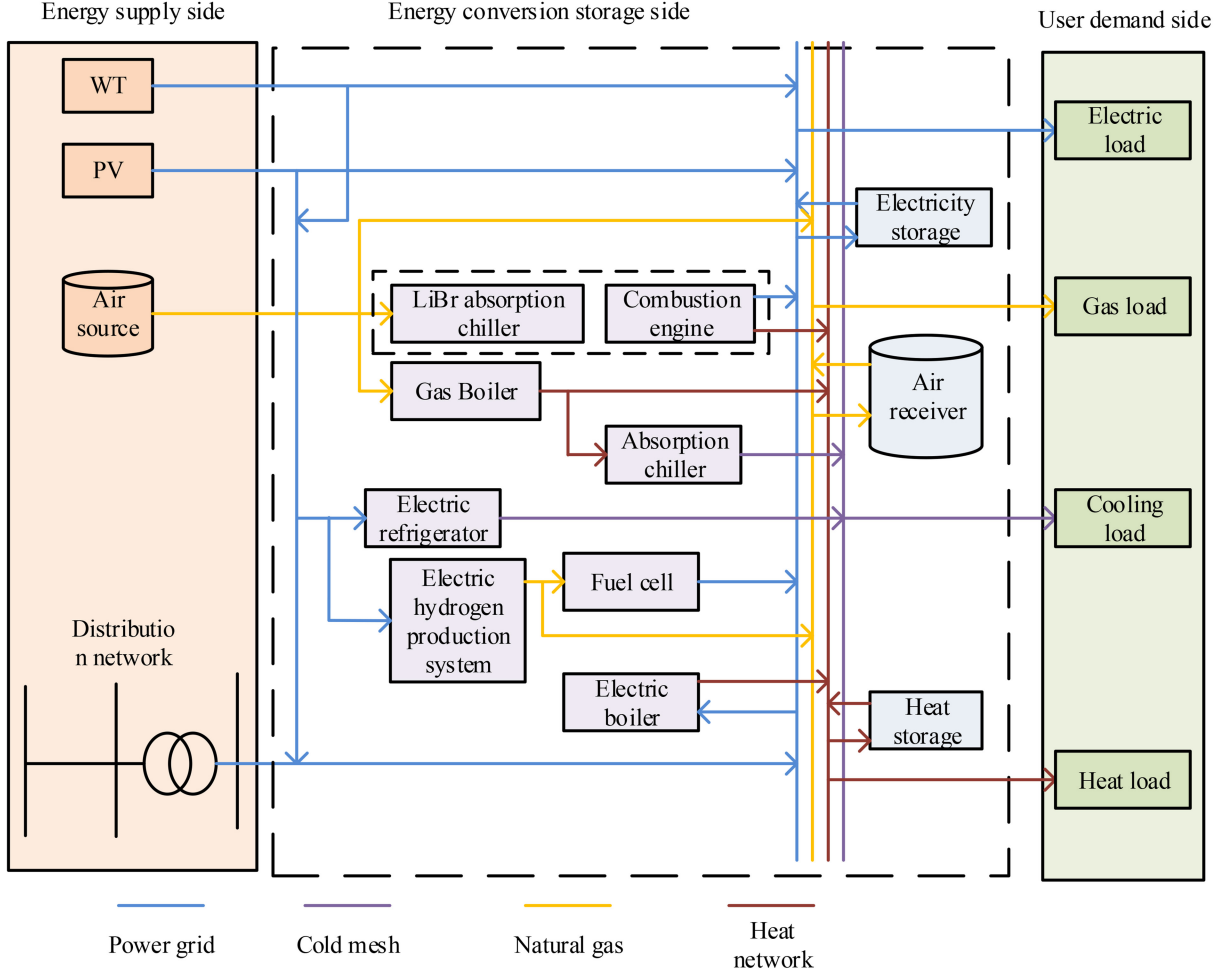
Figure 1. Operating structure of comprehensive energy microgrid.

boiler, electric refrigerator, absorption refrigerant, NG network, electric energy storage (EES), P2G, wind and photovoltaic power generation (PPG) models. In IES, the working efficiency of micro gas turbines is higher, and its mathematical model is formula (1) [17]–[19].

$$
\begin{cases}
P_{\mathrm{MT}}(t) = \dfrac{H_{\mathrm{MT}}(t)\eta^{\mathrm{MT}}}{(1-\eta^{\mathrm{MT}})\eta_{\mathrm{res}}^{\mathrm{MT}}K_{h0}} \\
\eta_{\mathrm{res}}^{\mathrm{MT}} = \dfrac{T_1 - T_2}{T_1 - T_0} \\
Q_{\mathrm{MT}} = \dfrac{\sum H_{\mathrm{MT}}(t)\Delta t}{(1-\eta^{\mathrm{MT}})\eta_{\mathrm{res}}^{\mathrm{MT}}K_{h0}H}
\end{cases}
\tag{1}
$$

In (1), $P_{\mathrm{MT}}(t)$ and $H_{\mathrm{MT}}(t)$ represent the electrical and thermal power output of the micro-gas-turbine at t-time. η^{MT} represents the conversion ratio of the micro gas turbine. $\eta_{\mathrm{res}}^{\mathrm{MT}}$ is the waste heat recovery ratio. K_{h0} is the heating coefficient. T_1 is the environmental coefficient where Unit 1 is located, and T_2 is the environmental coefficient where Unit 2 is located. T_0 is the real-time environment temperature where the unit is located. $Q_{\mathrm{MT}}(t)$ represents the NG wastage of the micro-gas-turbine at t-time, and H is the heat value released by the condensation of water vapour generated by the complete combustion of NG into water. A gas boiler serves as a supplementary output when that output is insufficient. The device directly heats the system through high-temperature

steam generated by combustion, and its mathematical model is (2).

$$
\begin{cases}
P_{\mathrm{GB}}(t) = \eta_{\mathrm{GB}}P_{\mathrm{GB.gas}}(t) \\
H_{\mathrm{GB}}(t) = P_{\mathrm{GB}}(t)\Delta t \\
Q_{\mathrm{GB}}(t) = \dfrac{P_{\mathrm{GB.gas}}(t)\times\Delta t}{\mathrm{GHV}}
\end{cases}
\tag{2}
$$

In (2), $P_{\mathrm{GB}}(t)$ and $P_{\mathrm{GB,gas}}(t)$ mean the thermal power output and gas input power of the gas boiler at time t. η_{GB} is the gas to heat conversion ratio of a gas fired boiler. $H_{\mathrm{GB}}(t)$ refers to the heat production. $Q_{\mathrm{GB}}(t)$ is the NG usage. GHV represents the low calorific value of NG. Electric boiler is a commonly used electric heating conversion equipment that could practically lift the flexibility of energy systems. It can serve as both a heat source for the thermal system and a load for the power system. Equation (3) is the calculation.

$$
\begin{cases}
P_{\mathrm{EB}}(t) = P_{\mathrm{CE}}(t)\eta_{\mathrm{EB}} \\
H_{\mathrm{EB}}(t) = P_{\mathrm{EB}}(t)\Delta t
\end{cases}
\tag{3}
$$

In (3), $P_{\mathrm{EB}}(t)$ and $P_{\mathrm{CE}}(t)$ represent the thermal output power and power consumption of the electric boiler at time-t. η_{EB} represents its electric heating
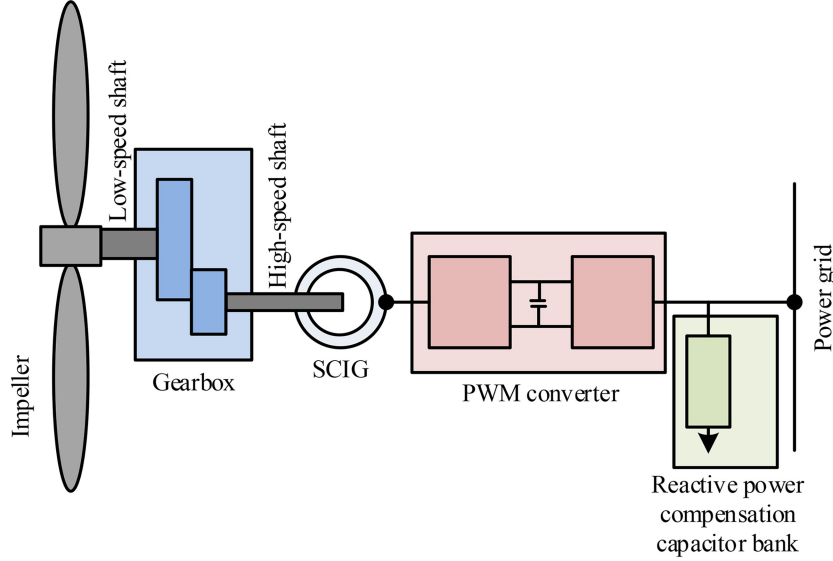
Figure 2. Wind turbine system.

conversion efficiency. $H_{\mathrm{EB}}(t)$ is the heating capacity. Electric refrigeration units are mainly responsible for improving the overall economic operation level of the system, and their cooling capacity is in direct proportion to the power input. While the electricity price efficiency is high, the cooling load can be output. As expressed in (4).

$$\begin{cases} P_{\mathrm{ER}}(t) = Q_{\mathrm{ER}}(t) \cdot COP_{\mathrm{ER}} \\ C_{\mathrm{ER}}(t) = P_{\mathrm{ER}}(t)\,\Delta t \end{cases} \tag{4}$$

In (4), $P_{\mathrm{ER}}(t)$ is the cooling load output and $Q_{\mathrm{ER}}(t)$ is the electrical load input of the electric refrigeration unit at time-t. $\mathrm{CO}P_{\mathrm{ER}}$ is the electric cooling conversion coefficient. $C_{\mathrm{ER}}(t)$ is the cooling capacity. Wind power generation is an important energy supply part of IES. The overall structure of wind power generation is divided into two parts, namely, wind turbines and generators, as shown in Fig. 2.

The probability density model of wind speed for wind turbines can be predicted using the Weibull distribution model, and information, such as expected wind energy density can be calculated based on the prediction. The mathematical formula between the output power of a wind turbine and the input wind speed can be expressed by (5) [20], [21].

$$P_{\mathrm{WT}}(t) = \begin{cases} P_{W\_\mathrm{rated}}(t) & v_r < v < v_{\mathrm{co}} \\ P_N(t)\frac{v - v_{\mathrm{ci}}}{v_r - v_{\mathrm{ci}}} & v_{\mathrm{ci}} < v < v_N \\ 0 & 0 < v < v_{\mathrm{ci}}, v < v_{\mathrm{co}} \end{cases} \tag{5}$$

In (5), c is the standard parameter of the Weibull distribution. The NG network model is one of the energy supply models of IES, and there are many similarities between the current NG network and the power output network. It includes micro gas turbines, compressors, and gas storage tanks. The gas well is its energy source, and the operation process of the NG network starts from the gas

well. The gas pipeline transports energy to be converted and stored as well as to meet the demand of users. When NG is transported, energy loss occurs, which causes a drop in the gas pressure within the pipeline. At this time, the compressor can adjust the pressure inside the NG pipeline by compressed NG. Gas storage tanks are comparable to electrical energy storage equipment in the power grid system, in terms of their function. NG may be stored when its economic benefits exceed a certain threshold. However, when the benefits fall below a critical level, the stored NG will be transported to the NG system to enhance its economic benefits. The important components of the NG system include NG pipelines and compressors, among which the NG pipeline mainly refers to its flow model, which is displayed in (6).

$$\begin{cases} Q_{L,\mathrm{mn}} = \mathrm{sgn}_p\,(p_n, p_m)\,k_{\mathrm{mn}}\sqrt{\mathrm{sgn}_p\,(p_n, p_m)\,(p_n^2, p_m^2)} \\ \mathrm{sgn}_p\,(p_n, p_m) = \begin{cases} 1, & p_n > p_m \\ -1, & p_n \ge p_m \end{cases} \end{cases} \tag{6}$$

In (6), $Q_{L,\mathrm{mn}}$ is the gas flow value of NG pipeline-L from the first node m to the end node n. sgn_p represents the direction of NG transmission. p_m, p_n represent the pressure value of network node m, n. k_{mn} represents the pipeline constant. Equation (7) is the mathematical model of the compressor.

$$\begin{cases} Q_{L,\mathrm{mn}} \le k_{\mathrm{mn}}\sqrt{(p_n^2, p_m^2)} \\ p_m \le \lambda_c \cdot p_n \end{cases} \tag{7}$$

In (7), λ_c represents the compression ratio of the compressor. EES systems include electrochemical, electromagnetic, and physical energy storage. Because of its extensive range of applications and fast operation speed, IES utilises the electrochemical energy storage system. Equation (8) shows the mathematical model of
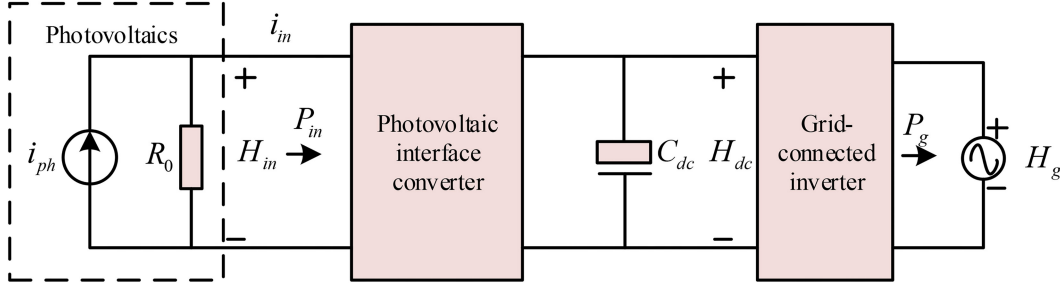
Figure 3. Equivalent circuit diagram of PPG.

this technology.

$$P_{\text{BS}}(t+1) = P_{\text{BS}}(t) + \alpha_c P_{\text{BR}}(t) - \alpha_d P_{\text{BR}}(t) \quad (8)$$

In (8), $P_{\text{BS}}(t) P_{\text{BR}}(t)$ are the charging and discharging power of the EES device at time t. α_c, α_d represent the charging & discharging coefficients. P2G technology is an emerging technology that can provide auxiliary services for IES and promote the coupling and complementarity of multiple energy sources. The operating formula of P2G devices in IES is (9).

$$Q_{P2G,r} = \frac{n_{P2G,r} P_{P2G,r}}{\text{GHV}} \quad r = 1, 2, \ldots, N_{P2G} \quad (9)$$

In (9), $Q_{P2G,r}$, $\eta_{P2G,r}$, and $P_{P2G,r}$, respectively, represent the output NG flow rate, electricity conversion efficiency, and consumed electricity power of device r in the P2G device. N_{P2G} represents the total number of P2G devices in IES. PPG is an important energy supply part besides wind power generation, and its basic structure is Fig. 3.

PPG is a technology that utilises the photovoltaic effect to convert light energy into electricity, mainly composed of solar panels, inverters, and controllers. To improve the output voltage of the PPG system, it is necessary to connect the photovoltaic cells in series to form a photovoltaic array. The power output expression of the V–A characteristic curve of the system's output energy is (10) [22].

$$P_{\text{PV}}(t) = P_{\text{STC}}(t) \frac{I_{\text{ING}}}{I_{\text{STC}}} [1 + \alpha (T_c - T_r)] \quad (10)$$

In (10), $P_{\text{PV}}(t)$ and $P_{\text{STC}}(t)$, respectively, refer to the actual and max-output values of the PPG unit. I_{ING} and I_{STC} represent the actual and standard values of the external light intensity received by the PPG unit. T_c is the correlation coefficient between the PPG output power and the external environmental temperature. α represents the actual temperature of the photovoltaic generator unit battery. T_r is the reference temperature value of the photovoltaic generator unit battery. To achieve the best economic benefits of IES, it is necessary to adjust the output of each subsystem in the IES system according to user needs.

3.2 Improved Whale Algorithm Based on Reverse Learning

To achieve the max economic benefits of IES and achieve mutual collaboration among various subsystems of IES, it is necessary to optimise the output parameters of each system. WOA has the advantage of fast convergence speed and was formally put forward in 2016. It simulates the predatory behaviour of whales in the ocean, and its process is Fig. 4 [23], [24].

If the whale population contains N whales and the problem has D dimensions, then each whale in the whale population corresponds to a position in D. The location of the whale that preys the most in the whale group is the optimum to the issue. WOA is mainly divided into three stages, namely, encircling prey, preying on prey, and searching for prey. During the encircling stage, whales will first observe the area where the prey is located, and then engage in encircling activities. At this time, the leading whale is the optimal solution, while other individuals continuously approach it and update their position information in real time. Therefore, WOA needs to first calculate the distance between each individual and the optimal solution, that is, the positional distance between the individual in the school and the lead whale, as shown in (11).

$$\begin{cases} \overrightarrow{X}(b+1) = X*(b) - \overrightarrow{A} \cdot \overrightarrow{D} \\ \overrightarrow{D} = \left| \overrightarrow{C} \cdot X*(b) - \overrightarrow{X}(b) \right| \\ \overrightarrow{A} = 2a \cdot \overrightarrow{r} - a \\ \overrightarrow{C} = 2 \cdot \overrightarrow{r} \end{cases} \quad (11)$$

In (11), b represents the iterations. $X*(t)$ and $\overrightarrow{X}(t)$ are the position vectors of the optimal solution and current position. $\overrightarrow{A}, \overrightarrow{C}$ represent the coefficient. a represents the parameter, and $\overrightarrow{r}$ represents a random vector. After completing the encirclement stage, whales enter the predation stage, which is divided into two situations. The first situation is to contract the encirclement net for predation. In this case, $\overrightarrow{A}$ takes a value within $[-1, 1]$, and each whale moves towards the lead whale, updating its position in real-time as it moves. The second scenario is spiral bubble predation, in which each individual calculates its distance to the optimal solution position and sprays bubbles upwards in the form of a spiral ascent. At this
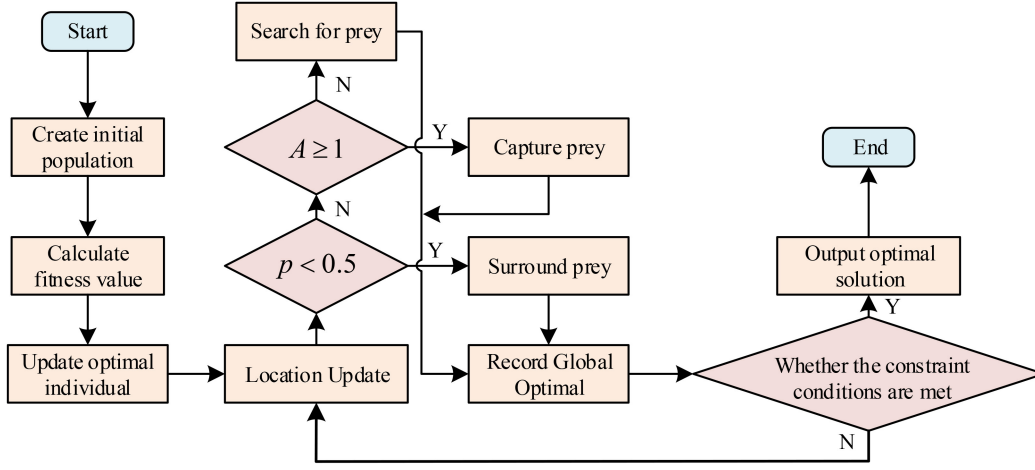
Figure 4. WOA flowchart.

point, the fish approached the position of the leading whale gradually. When whales prey, the probability of both situations occurring is equal, both of which are 50%. The mathematical model of whale hunting behaviour is (12).

$$\overrightarrow{X}(b+1) = \begin{cases} X*(b) - \overrightarrow{A} \cdot \overrightarrow{D} & \text{if } \rho \leq 0.5 \\ \overrightarrow{D} \cdot e^{bl} \cdot \cos(2\pi l) + X*(b) & \text{if } \rho \geq 0.5 \end{cases} \quad (12)$$

In (12), $\overrightarrow{D'} = \left| X*(b) - \overrightarrow{X}(b) \right|$ refers to the distance from the whale to its prey, b represents a constant, and l is a random no. within $[-1, 1]$. After completing the predation, the fish school will start searching for prey again. At this stage, individuals will no longer approach the lead whale and start randomly searching for prey. The behaviour model of this stage is (13).

$$\begin{cases} \overrightarrow{D} = \left| \overrightarrow{C} \cdot \overrightarrow{X}_r - \overrightarrow{X} \right| \\ \overrightarrow{X}(b+1) = \overrightarrow{X}_r - \overrightarrow{A} \cdot \overrightarrow{D} \end{cases} \quad (13)$$

In (13), $\overrightarrow{X}_r$ represents the random position vector for population selection. WOA is iteratively calculated from an initial generation. If the selected initial generation is located very close to the optimal solution, it can improve the overall running speed and convergence rate of the algorithm. The reverse learning mechanism can help the algorithm select the initial generation position closer to the optimal solution. Therefore, the reverse learning mechanism is proposed to improve WOA to improve the running speed and convergence rate of WOA. The initial generation of WOA in the D-dimension is $X_i = \{x_{i,1}, x_{i,2}, \ldots, x_{i,D}\}$, then the reverse generation is $X'_i = \{x'_{i,1}, x'_{i,2}, \ldots, x'_{i,D}\}$, and the expression for the reverse generation is (14).

$$x'_{i,j} = (x_{\max,D} + x_{\min,D}) - x_{i,j} \quad (14)$$

In (14), i represents the feasible solution numbers in the search-space, and j represents the dimension of feasible solutions in the search space. To enhance the variety of search and cut down the impact of diversity, an exponential

decreasing function is proposed to optimise the parameter a in WOA. The calculation method is (15).

$$a = a_{\min} + (a_{\max} - a_{\min}) \times e^{\frac{-1}{\text{Max\_iter} - 10}} \quad (15)$$

The process of improving WOA is Fig. 5.

The initial population generates N initial positions in the solution space, and the reverse population also generates N reverse initial positions. After initialising WOA parameters, calculate the fitness values of $2N$ initial positions, and take the current best as the leader whale of the population. After determining the lead whale, it begins the cycle of WOA. Equation (12) selects one predatory behaviour for position updating, which is updated using (13) after capturing prey. Upon the completion of enhancing WOA, it is imperative to reassess the algorithm's limitations, particularly the constraints on interactive transmission power between the subsystem and the primary network, as depicted in (16).

$$\begin{cases} P_{\text{PE,min}} \leq P_{\text{PE}}(t) \leq P_{\text{PE,max}} \\ P_{\text{SE,min}} \leq P_{\text{SE}}(t) \leq P_{\text{SE,max}} \end{cases} \quad (16)$$

In (16), $P_{\text{PE,min}}$ and $P_{\text{PE,max}}$ represent the minimum and maximum power of purchased electricity from the distribution network. $P_{\text{SE,min}}$ and $P_{\text{SE,max}}$ represent the minimum and maximum power to sell electricity to the distribution network. The second constraint is the air source point, as shown in (17).

$$\begin{cases} Q_{S,\min} \leq Q_{\text{EB}}(t) \leq Q_{S,\max} \\ Q_{S,\min} \leq Q_{\text{MT}}(t) \leq Q_{S,\max} \end{cases} \quad (17)$$

In (17), $Q_{S,\max}$ and $Q_{S,\min}$ represent the maximum and minimum amount of NG purchased from the NG network. Finally, there is the node pressure constraint, as shown in (18).

$$\begin{cases} P_{n,\min} \leq P_n(t) \leq P_{n,\max} \\ P_{m,\min} \leq P_m(t) \leq P_{m,\max} \end{cases} \quad (18)$$
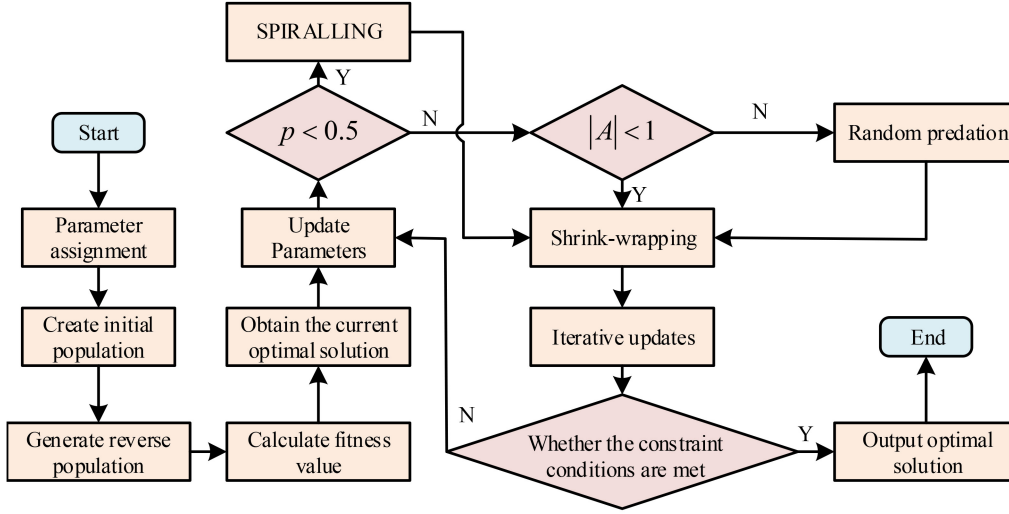
Figure 5. Improved WOA algorithm process.
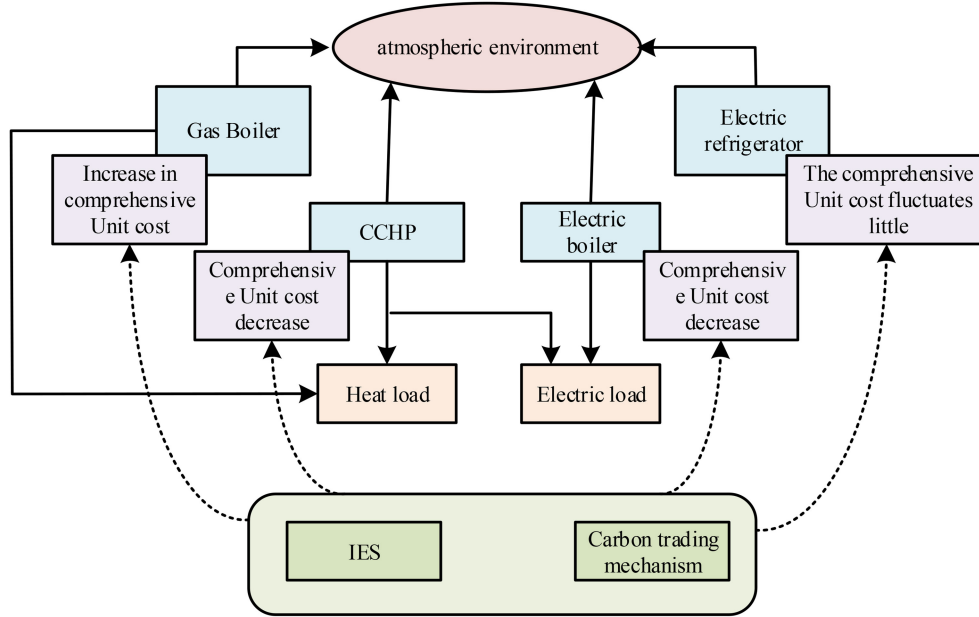
Figure 6. Impact of carbon trading mechanism on IES.

In (18), $P_{m,\min}$ and $P_{m,\max}$ are the lower and upper pressure limit of head node m. $P_{n,\min}$ and $P_{n,\max}$ are the lower and upper pressure limit of end node n. In addition to the constraints, it is also necessary to calculate the operating costs of each system, as shown in (19).

$$f_{\mathrm{oc}} = \sum \left[f_{\mathrm{GAS}}\left(t\right) + f_{\mathrm{PSE}}\left(t\right) + f_{\mathrm{MU}}\left(t\right) \right] \Delta \mathrm{t} \qquad (19)$$

In (19), f_{oc} represents the total maintenance cost of the system. $f_{\mathrm{GAS}}\left(t\right)$ represents the NG purchase cost in period t. $f_{\mathrm{PSE}}\left(t\right)$ represents the cost of purchasing or selling electricity from the distribution network in period t. $f_{\mathrm{MU}}\left(t\right)$ represents the maintenance cost of each unit in period t. Studying the best scheduling behaviour of IES also needs to consider the effect of LC-Eco on IES. After introducing a carbon trading mechanism (CTM), an additional penalty cost needs to be considered in the

parameters of IES. Therefore, on the premise of meeting user needs, the system will prioritise CCHP and electric boiler units, and the effect of CTM on IES is Fig. 6.

4. Simulation Experiment Results

To confirm the effectiveness of the reverse learning mechanism in enhancing WOA, a study was performed. Energy data from a specific region in 2020 was applied as a training set. A computer was employed for the comparison of running speed, convergence speed, system load, fitness, operating cost, and unit output of improved WOA, WOA, and linear programming. The computer used a Windows 7 system, with an Inter (R) Core (TM) i5-4460 processor and a 3.02 Hz CPU. The study was conducted in this environment. The comparison was conducted using Matable7.0 software. The results are shown in Fig. 7.
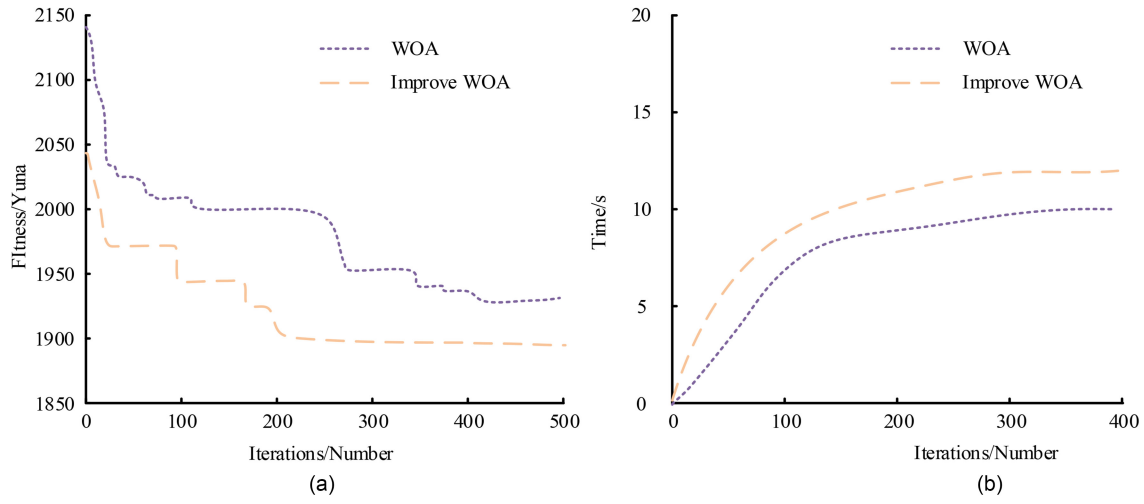
Figure 7. Performance comparison between improved WOA and WOA: (a) convergence speed comparison and (b) running speed comparison.
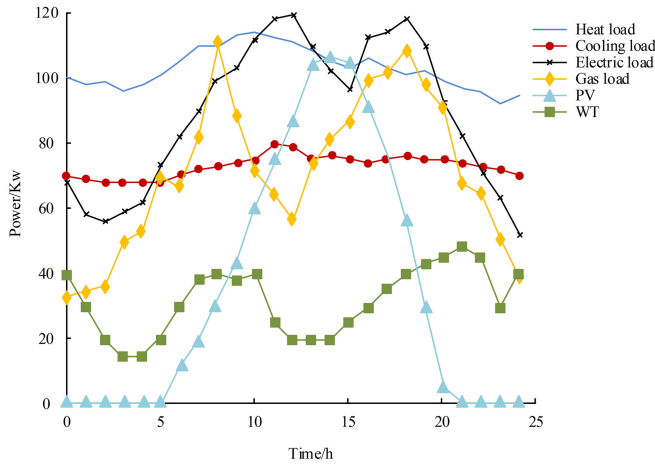
Figure 8. Daily load and solar output prediction.

Figure 7 shows the performance comparison of two algorithms: WOA and its improved version. Figure 7(a) shows that the enhanced WOA achieves its optimal solution in about 200 iterations, whereas the standard WOA requires 400 iterations to reach the same. The total cost of IES in the improved algorithm is 1,900 yuan, compared to 1,940 yuan in the original WOA. In Fig. 7(b), the execution speeds of the two algorithms were similar during the initial iteration. But as iterations grow, performance differences begin to manifest. Specifically, after 400 iterations, the improved WOA took 12.84 s, while the original WOA took 9.86 s. This study indicates that the improving WOA is effective. For IES energy scheduling, regional user demand is a key consideration. Predictions were made for daily wind power, solar energy production, and other system loads in specific regions, with detailed results shown in Fig. 8.

In Fig. 8, during the day, the maximum photovoltaic output can reach over 100 kW, and the cooling load output is relatively stable at around 70 kW throughout the entire time period. The heat load has a higher output during the noon period, reaching over 110 kW. The output in the early

morning is relatively low, around 90 kW. The electrical and gas loads are related to the daily life of the people in the area, with the highest electrical load reaching 120 kW and the lowest being 50 kW. The maximum gas load is 110 kW, and the minimum is 55 kW. The wind turbine output in this area is relatively low, with a maximum of around 45 kW and a minimum of only 15 kW. The purchase or sale of IES from the distribution network in the region can be classified into peak, valley, and normal periods, based on daily load forecasting, with different prices assigned to each period. To demonstrate the potential of CTM in optimising the scheduling of IES LC-Eco, this study employs an improved WOA algorithm to estimate the variation in the fitness value, total operating cost, and CE of IES under different conditions. Figure 9 shows the results.

Figure 9(a) shows the optimisation iteration results of the algorithm in different scenarios. The system without CTM converges in the 140th iteration, and its fitness value is the highest, 1,940 yuan. The system with traditional CTM converges in the 200th iteration, and its fitness value is 1,890 yuan. The system that introduced a tiered CTM converged in the 250th iteration, with a fitness value of 1,900 yuan. Figure 9(b) shows the optimal operating costs of the system in different conditions. Among the three scenarios, the system without introducing a CTM has the highest operating cost and CE. The system that introduces traditional CTMs has the lowest operating cost. The system that introduces a tiered CTM has the lowest CE. After determining the impact of introducing different CTMs on IES, the study investigated the output of each unit under different scenarios, as shown in Fig. 10.

Figure 10(a) shows the output of each IES unit without introducing a CTM. There is a significant difference in it, with the highest output of the gas furnace reaching 300 kW and the lowest output of the electric refrigeration unit being only 20 kW. Figure 10(b) shows that under the introduction of traditional CTM. The output of the gas furnace has decreased, and the peak output has decreased by about 30 kW. The output of the CCHP unit has increased, while the other units have remained basically
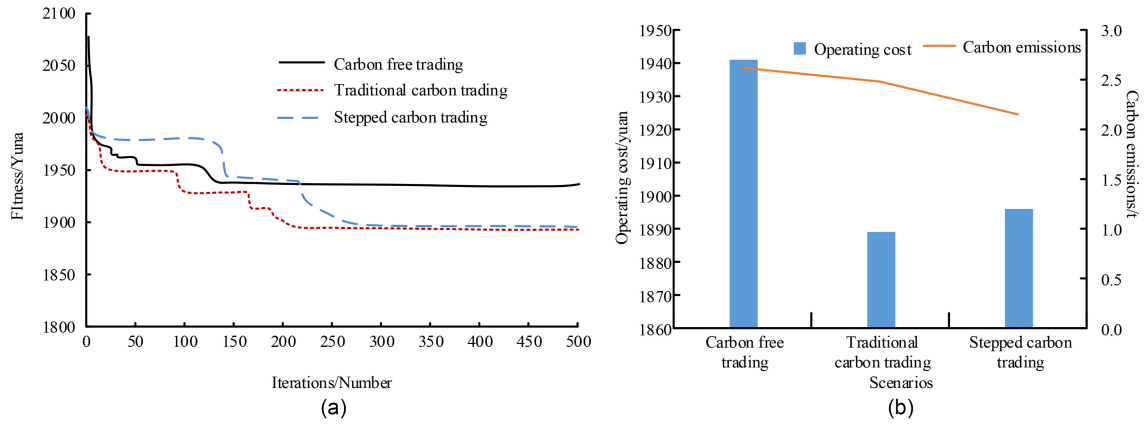
Figure 9. Optimisation iteration and comprehensive operating costs in different scenarios: (a) iterative optimisation in different scenarios and (b) operating costs and carbon emissions for different scenarios.
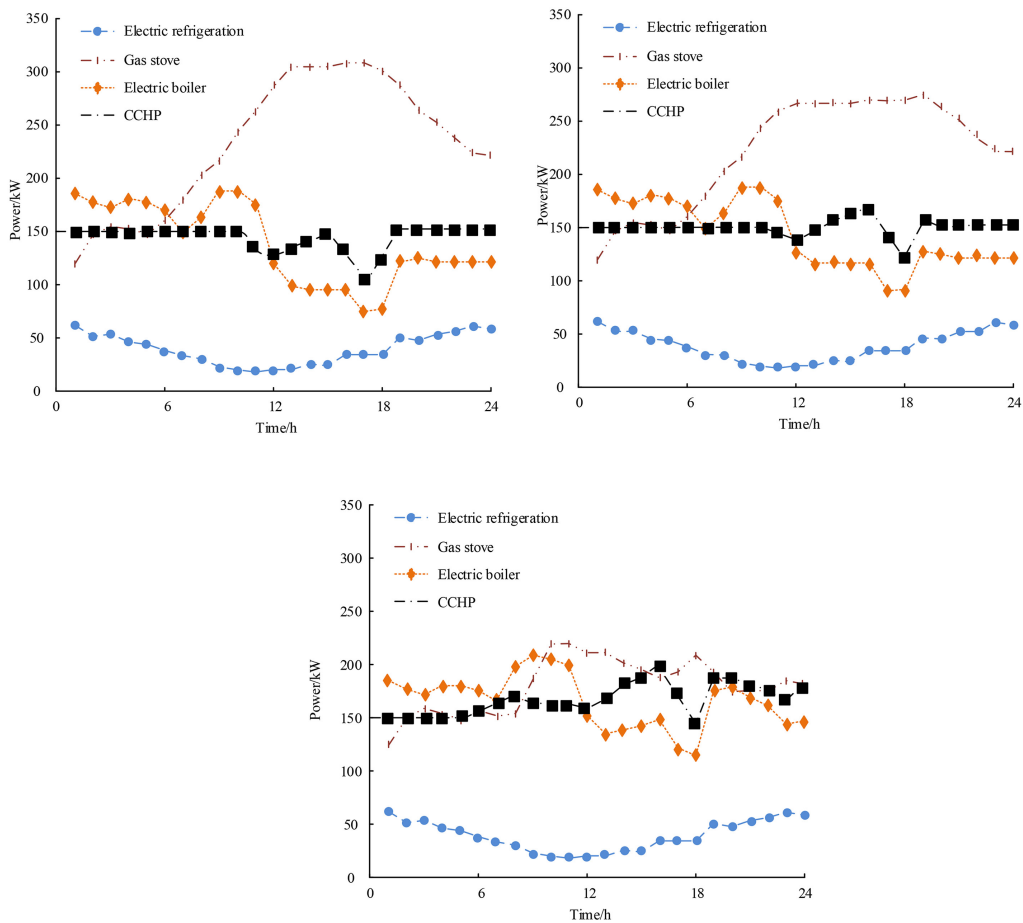
Figure 10. Output of each unit in different scenarios: (a) carbon free trading mechanism; (b) carbon free trading mechanism; and (c) carbon free trading mechanism.

unchanged. Figure 10(c) shows that of a tiered CTM. The output of the gas furnace has significantly decreased, with a maximum of only 220 kW. The output of the electric boiler and CCHP units has also increased. The study also explored the EES devices impact on the operating status of IES, as shown in Fig. 11.

Figure 11(a) shows the IES without calculating the CE of EES equipment. In this scenario, as the carbon trading price increases, the output of gas furnaces and electric refrigerators gradually decreases, while the output of CCHP and electric furnaces begins to increase. When the carbon trading price is 48 yuan/t, the gas furnace and electric furnace stop operating, and the system heating is entirely responsible for CCHP and electric furnace. When the price is 32 yuan/t, the EES equipment starts to operate and increases. When the price increases to 108 yuan/t, the
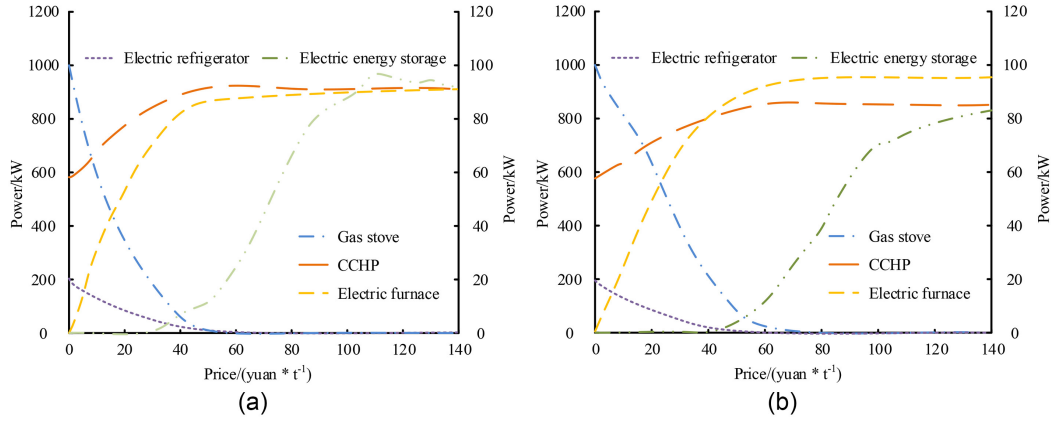
Figure 11. Operating status of IES in different scenarios: (a) the output of each unit without introducing carbon trading mechanism and (b) the output of each unit without introducing carbon trading mechanism.
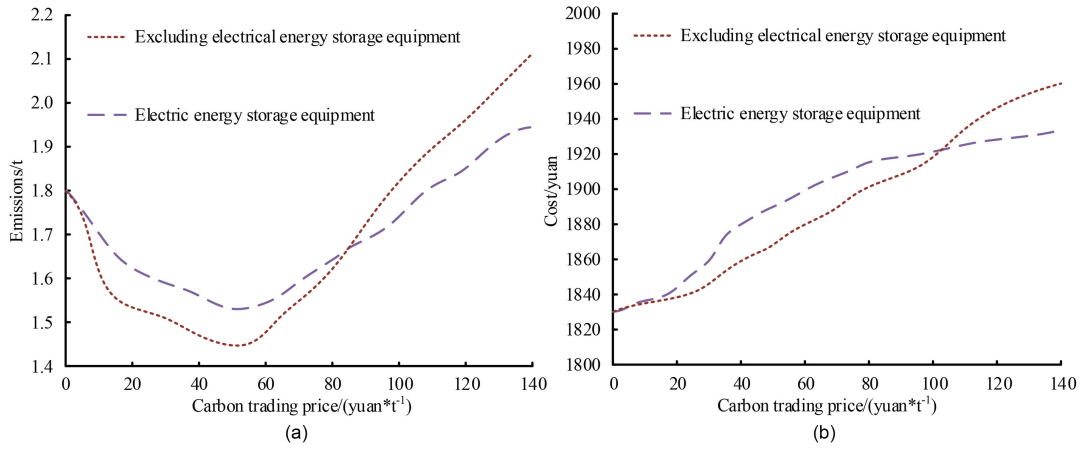
Figure 12. Changes in CE and operating costs of the system under different scenarios: (a) changes in carbon emissions and (b) changes in operating costs.

output of EES equipment begins to decline. Figure 11(b) shows the IES for calculating the CE of EES equipment. In this scenario, when that price increases to 63 yuan/t, the gas furnace stops operating, and at this time, the output of CCHP reaches its maximum. When that increases to 43 yuan/t, the EES equipment begins to operate and continues to increase its weight. Once it rises to 102 yuan/t, the EES equipment output still rises, yet the growth rate starts slowing down, causing the CCHP output to decrease. Finally, the study compared the changes in CE and system operating costs under two scenarios, as listed in Fig. 12.

Figure 12(a) shows a comparison of CE. When the carbon trading price is 52 yuan/t, the system without EES equipment reaches the min CE. When the price is 55 yuan/t, the system of the energy storage equipment reaches the minimum CE. When it is 84 yuan/t, the CE of the two scenarios are equal. Prior to this, the CE of electricity storage devices were lower than those of electricity storage devices. Figure 12(b) shows the initial stage of comparing the system operating costs. In both scenarios, the operating costs of the system are almost the same. When that is 9 yuan/t, the operating costs of the electricity storage equipment begin to be higher than those of the non-electricity storage equipment. While it

is 102 yuan/t, the costs are consistent. If the price keeps increasing, the cost of the system without EES equipment would eventually surpass the operating cost of the EES equipment system.

5. Conclusion

To study the output of each unit in IES's LC-Eco optimal dispatching model and optimise the model, reverse learning mechanism is proposed to improve WOA. Moreover, the improved WOA was utilised to lift the model's parameters. The results show that the improvement of WOA through research is effective and feasible, with a 50% increase in convergence speed, and the convergence was completed only in the 200th iteration. After introducing a tiered CTM, the improved WOA has the lowest CE, at 2.15 t. After introducing the traditional CTM, the system has the lowest operating cost of 1,889 yuan. After introducing the traditional CTM, the output of the gas furnace decreased by about 30 kW, which was supplemented by CCHP. After introducing a stepped CTM, the output of the gas furnace decreased by 80 kW, which was supplemented by electric boilers and CCHP. After introducing and calculating the CE of EES equipment, the operating cost of the system will

10

decrease when the carbon trading price reaches 102 yuan/t. The study explored the use of improved WOA to optimise the LC-Eco scheduling model of IES. In this model, the carbon TM is not linked to the electricity market, and further research can be conducted on the correlation between CTMs and electricity market transactions. The proposed model in the study heavily relies on the accuracy and correlation of WOA adjustment. Nevertheless, its applicability to all IES scenarios or regions with different energy distributions remains doubtful.

6. Funding

References

[1] Z. Yu, L. Shen, C. Shuai, Y. Tan, Y. Ren, and Y. Wu, Is the low-carbon economy efficient in terms of sustainable development? A global perspective, *Sustainable Development*, *27*(1), 2019, 130–152.

[2] L.Y. Zhang, M.L. Tseng, C.H. Wang, C. Xiao, and T. Fei, Low-carbon cold chain logistics using ribonucleic acid-ant colony optimization algorithm, *Journal of Cleaner Production*, 233, 2019, 169–180.

[3] K. Jain and A. Saxena, Simulation on supplier side bidding strategy at day-ahead electricity market using ant lion optimizer, *Journal of Computational and Cognitive Engineering*, *2*(1), 2023, 17–27.

[4] G.N. Sakalis, G.J. Tzortzis, and C.A. Frangopoulos, Synthesis, design and operation optimization of a combined cycle integrated energy system including optimization of the seasonal speed of a VLCC, *Proceedings of the Institution of Mechanical Engineers, Part M: Journal of Engineering for the Maritime Environment*, *235*(1), 2021, 41–67.

[5] J. Yuan, Y. Li, X. Luo, L. Li, and C. Li, Regional integrated energy system schemes selection based on risk expectation and Mahalanobis-Taguchi system, *Journal of Intelligent and Fuzzy Systems*, *40*(6), 2021, 1–18.

[6] X. Gao and W. Liu, Optimal device capacity planning and strategy determination in an integrated energy system to promoting IES integration considering reliability value, *IET Generation Transmission & Distribution*, *15*(6), 2021, 2356–2370.

[7] J. Su, H.D. Chiang, Y. Zeng, and N Zhou, Toward complete characterization of the steady-state security region for the electricity-gas integrated energy system, *IEEE Transactions on Smart Grid*, *12*(4), 2021, 3004–3015.

[8] H. Liu, S. Tian, X. Wang, Y. Cao, and Y. Li, Optimal planning design of a district-level integrated energy system considering the impacts of multi-dimensional uncertainties: A multi-objective interval optimization method, *IEEE Access*, *9*(1), 2021, 26278–26289.

[9] Q. Guo, L. Gao, X. Chu, and H. Sun, Parameter identification for static var compensator model using sensitivity analysis and improved whale optimization algorithm, *CSEE Journal of Power and Energy Systems*, *8*(2), 2022, 535–547.

[10] O.O. Obadina, M.A. Thaha, K. Althoefer, and M.H. Shaheed, Dynamic characterization of a master-slave robotic manipulator using a hybrid grey wolf–whale optimization algorithm, *Journal of Vibration and Control*, *28*(15/16), 2021, 1992–2003.

[11] R. Gupta, M.A. Alam, and P. Agarwal, Whale optimization algorithm fused with SVM to detect stress in EEG signals, *Intelligent Decision Technologies*, *15*(1), 2021, 87–97.

[12] M.A. Kahya, S.A. Altamir, and Z.Y. Algamal, Improving whale optimization algorithm for feature selection with a time-varying transfer function, *Numerical Algebra, Control, Optimization*, *11*(1), 2021, 87–98.

[13] K. Heraguemi, Whale optimization algorithm for solving association rule mining issue, *IJCDS Journal*, *10*(1), 2021, 332–342.

[14] R. Wang, S. Cheng, X. Zuo, and Y. Liu, Optimal management of multi stakeholder integrated energy system considering dual incentive demand response and carbon trading mechanism, *International Journal of Energy Research*, *46*(5), 2022, 6246–6263.

[15] J. Jia, G. Zang, and M.C. Paul, Energy, exergy, and economic (3E) evaluation of a CCHP system with biomass gasifier, solid oxide fuel cells, micro-gas turbine, and absorption chiller, *International Journal of Energy Research*, 45(10), 2021, 15182–15199.

[16] Y. Wang, L. Wang, R.F. Hu, L.X. Kong, and J. Cheng, Effects of sampling frequency on the proper orthogonal decomposition based reconstruction of a wind turbine wake, *IET Renewable Power Generation*, *15*(13), 2021, 2956–2970.

[17] L. Xiong, X. Zhang, and Y. Chen, Experimental verification of volt-ampere characteristic curve for a memristor-based chaotic circuit, *Circuit World*, *46*(1), 2019, 13–24.

[18] A. Mohammadbeigi, A. Maroosi, and M. Hemmati, Optimal chiller loading for energy conservation using a hybrid whale optimization algorithm based on population membrane systems, *International Journal of Modelling & Simulation*, *42*(1/2), 2022, 101–116.

[19] A. Qi, D. Zhao, F. Yu, A.A. Heidari, H. Chen, and L. Xiao, Directional mutation and crossover for immature performance of whale algorithm with application to engineering optimization, *Journal of Computational Design and Engineering*, *9*(2), 2022, 519–563.

[20] K. Asghari, M. Masdari, F.S. Gharehchopogh, and R. Saneifard, A chaotic and hybrid gray wolf-whale algorithm for solving continuous optimization problems, *Progress in Artificial Intelligence*, *10*(3), 2021, 349–374.

[21] F. Jiang, L. Wang, and L. Bai, An improved whale algorithm and its application in truss optimization, *Journal of Bionic Engineering*, *18*, 2021, 721–732.

[22] J. Luo, F. He, H. Li, X.T. Zeng, and Y. Liang, A novel whale optimisation algorithm with filtering disturbance and nonlinear step, *International Journal of Bio-Inspired Computation*, *20*(2), 2022, 71–81.

[23] S.R. Valayapalayam Kittusamy, M. Elhoseny, and S. Kathiresan, An enhanced whale optimization algorithm for vehicular communication networks, *International Journal of Communication Systems*, *35*(12), 2022, e3953.

[24] M. Li, G. Xu, Q. Lai, and J. Chen, A chaotic strategy-based quadratic opposition-based learning adaptive variable-speed whale optimization algorithm, *Mathematics and Computers in Simulation*, *193*, 2022, 71–99.

Biographies

Lin Jin received the Ph.D. degree in defense economics in 2010. She is working as an Associate Professor with the School of Finance and Trade, Wenzhou Business College. She has published more than 10 articles in Chinese core journals and foreign engineering index source journals. Her areas of interest include crisis management, public organisation management, and low-carbon economy.

Qian Sun a Ph.D. candidate at Zhongnan University of Economics and Law and an associate professor at Wuhan College. She has published two papers in Chinese Core Journals of Peking University and led two provincial research projects in China. Her research interests lie in international business and green economy.